Atmospheric Chemistry of BrO Radicals: Kinetics of the Reaction with $C_2H_5O_2$ Radicals at 233−333 K

Yosuke Sakamoto,[†,‡] Daisuke Yamano,[†] Tomoki Nakayama,[†,§] Satoshi Hashimoto,[†] Masahiro Kawasaki,[*,†] Timothy J. Wallington,[#] Shun Miyano,[%] Kenichi Tonokura,[%] and Kenshi Takahashi[$]

Department of Molecular Engineering, Kyoto University, Kyoto 615-8510, Japan, Ford Motor Company, RIC-2122, Dearborn, Michigan 48121-2053, Environment Science Center, The University of Tokyo, Tokyo 113-0033, Japan, and Pioneering Research Unit, Kyoto University, Gokasho, Uji 611-0011, Japan

Received: May 15, 2009; Revised Manuscript Received: July 22, 2009

Cavity ring-down spectroscopy was used to study the title reaction in 50−200 Torr of O_2 diluent at 233−333 K. There was no discernible effect of total pressure, and a rate constant of $k(BrO + C_2H_5O_2) = (3.8 \pm 1.7) \times 10^{-12}$ cm^3 molecule^{-1} s^{-1} was determined at 293 K in 150 Torr total pressure of O_2 diluent. The addition of 1.4×10^{17} molecules cm^{-3} of H_2O vapor had no measurable impact on $k(BrO + C_2H_5O_2)$ at 293 K and 150 Torr. The rate constant exhibited a negative temperature dependence and was described by $k(BrO + C_2H_5O_2) = 6.5 \times 10^{-13} \exp((505 \pm 570)/T)$ cm^3 molecule^{-1} s^{-1}. Results are discussed with respect to the atmospheric chemistry of BrO radicals.

1. Introduction

BrO radicals participate in ozone depletion in the troposphere and have been detected at levels up to 6.5 ppt at surface sites in Mace Head in Ireland,[1] 30 ppt in the Antarctic,[2] and 200 ppt at the Dead Sea.[3] Profiles measured during balloon flights at mid and high latitudes in the Northern Hemisphere indicate that BrO is present in the free troposphere at levels of approximately 0.5−2.0 ppt.[4] Read et al. reported a mean daytime maximum BrO concentration of about 2.5 ppt over an eight month observation period at Cape Verde.[5] The air mass arriving at Cape Verde is presumably representative of the surrounding open-ocean marine boundary layer. Atmospheric ozone is depleted via reactions 1−3:

$$Br + O_3 \rightarrow BrO + O_2 \quad (1)$$

$$BrO + HO_2 \rightarrow HOBr + O_2 \quad (2)$$

$$HOBr + h\nu \rightarrow Br + OH \quad (3)$$

von-Glasow et al. reported results of a modeling study indicating that BrO mixing levels of 0.1−2.0 ppt lead to decreases of zonal mean ozone mixing ratios of up to 18% over widespread areas and up to 40% regionally.[6] Yang et al. reported that the addition of bromine chemistry to an atmospheric model led to a 4−6% reduction in tropospheric ozone in the Northern Hemisphere and up to 30% reduction in tropospheric ozone in the Southern Hemisphere.[7] BrO radicals have an important impact on tropospheric ozone levels.

The concentration of organic peroxy radicals (RO_2, e.g., CH_3O_2, $C_2H_5O_2$, etc.) in the troposphere is comparable to that of HO_2 radicals.[8−10] Thus, if reaction 4 has a rate constant comparable to that of reaction 2, $k_2 = 2.4 \times 10^{-11}$ cm^3 molecule^{-1} s^{-1} at 298 K, reaction 4 would compete with reaction 2.

$$BrO + RO_2 \rightarrow \text{products} \quad (4)$$

To improve global atmospheric chemistry models, it is important to understand the kinetics and mechanism of reaction 4. Our present understanding of the chemistry of reactions of BrO radicals with organic peroxy radicals is restricted to the reaction with CH_3O_2 studied by Aranda et al.[11] and Enami et al.[12]

$$BrO + CH_3O_2 \rightarrow \text{products} \quad (5)$$

The reaction has a rate constant of approximately 6×10^{-12} cm^3 molecule^{-1} s^{-1} at 298 K[11,12] and displays a negative temperature dependence suggesting that it proceeds via the formation of a short-lived adduct.[12] If the reactivity of CH_3O_2 is representative of organic peroxy radicals (RO_2), then reaction 4 would compete for the available BrO radicals. At the present time, it is unclear whether reaction 5 provides a representative model for the more general reaction 4.

To improve our understanding of the atmospheric chemistry of BrO and peroxy radicals, we have extended our previous study of the reaction of BrO with CH_3O_2[12] to the next largest organic peroxy radical ($C_2H_5O_2$).

$$BrO + C_2H_5O_2 \rightarrow \text{products} \quad (6)$$

* Corresponding author. E-mail: kawasaki@moleng.kyoto-u.ac.jp.
† Department of Molecular Engineering, Kyoto University.
‡ Present address: Department of Chemical System Engineering, The University of Tokyo, Tokyo 113-0033, Japan.
§ Present address: Solar-Terrestrial Environment Laboratory, Nagoya University, Nagoya 464-8601, Japan.
# Ford Motor Company.
% The University of Tokyo.
$ Pioneering Research Unit, Kyoto University.

10.1021/jp904529a CCC: $40.75
Published on Web 09/01/2009

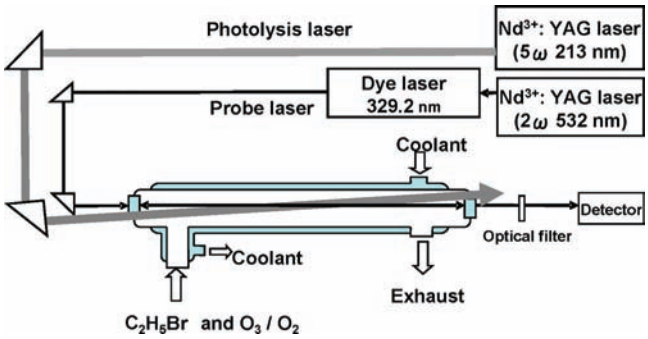

Figure 1. Experimental setup.

Possible reaction channels for reaction 6 are listed below with thermochemical data taken from Guha and Francisco,[13] IUPAC[14] and NASA/JPL[15] (BrOO is thermally unstable and will rapidly dissociate into Br + O_2):

		$\Delta_r H$ (kJ mol^{-1})	
$BrO + C_2H_5O_2$	$\rightarrow$ $C_2H_5O + BrOO$	0.2	(7)
	$\rightarrow$ $C_2H_5O + OBrO$	56.1	(8)
	$\rightarrow$ $HOBr + CH_3CHO_2$		(9)
	$\rightarrow$ $C_2H_5OBr + O_2$		(10)
	$\rightarrow$ $CH_3CHO + HOOBr$	-222.1	(11)
	$\rightarrow$ $CH_3CHO + O_2 + HBr$	-294.4	(12)

In this paper, we report kinetic data for the reaction of BrO with $C_2H_5O_2$ radicals at 233−333 K in 50−200 Torr total pressure of O_2 diluent, with and without added H_2O vapor, measured using a cavity ring-down spectroscopy (CRDS) and results are compared with ab initio and density functional theory calculations.

2. Experimental Section

To study the title reaction, C_2H_5Br was photodissociated at 213 nm to produce C_2H_5 and Br in the presence of O_2/O_3 mixtures.

$$C_2H_5Br + h\nu\,(213\text{ nm}) \rightarrow C_2H_5 + Br \qquad (13)$$

$$C_2H_5 + O_2 + M \rightarrow C_2H_5O_2 + M \qquad (14)$$

$$Br + O_3 \rightarrow BrO + O_2 \qquad (15)$$

Typical concentrations of O_3 and O_2 were $(2.5-7.0) \times 10^{15}$ and $(0.6-5) \times 10^{18}$ molecules cm^{-3}, respectively. Br and C_2H_5 are converted to BrO and $C_2H_5O_2$ within 1 ms and 1 μs, respectively. BrO radicals were monitored via their UV absorption at 329.1 nm using the CRDS apparatus shown in Figure 1. The system employed a photolysis laser (Spectra Physics, GCR-250) and a probe laser (Lambda Physik, Dye Laser SCANmate). The 213 nm output of the Nd^{3+}:YAG laser was used to dissociate C_2H_5Br to produce C_2H_5 and Br. To generate the fifth harmonic laser light at 213 nm, a temperature controlled BBO crystal was used to mix the fundamental and the fourth harmonic from the YAG laser. The typical laser intensity at 213 nm was 3 mJ pulse^{-1}.

After the photolysis laser pulse beam traversed the reaction cell, the probe laser pulse beam was injected nearly collinear to the axis of the photolysis laser through one of two high-reflectivity mirrors. The length of the reaction region was 0.40 ± 0.005 m. The cavity ring-down mirrors (Research Electro-Optics, 7.8 mm diameter, 1 m curvature) had a specified reflectivity of >0.999 and were mounted 1.04 m apart. Light leaking from the end mirror was detected by a photomultiplier tube (Hamamatsu Photonics, R212UH). The temporal decay of the light intensity was recorded using a digital oscilloscope (Pico, ADC-212, 12 bit) and transferred to a personal computer. In the presence of absorbing species, the light intensity within the cavity is given by:

$$I(t) = I_0 \exp(-t/\tau) = I_0 \exp(-t/\tau_0 - \sigma n c L_R t/L_C) \qquad (16)$$

where I_0 and $I(t)$ are light intensities at time 0 and t, τ is the cavity ring-down time in the presence of the absorbing species, τ_0 (typically 5 μs) is the cavity ring-down time in the absence of absorbing species, L_R is the length of the reaction region (0.40 m), L_C is the cavity length (1.04 m), c is the velocity of light, and n and σ are the concentration and absorption cross section of absorbing species, respectively. Each ring-down trace was digitized with a time resolution of 20 ns. Averages of 32 digitized traces were used to calculate ring-down rates, τ^{-1}.

A value of $\sigma_{BrO} = 1.2 \times 10^{-17}$ cm^2 molecule^{-1} at 329.1 nm was used to calculate the absolute concentration of BrO at 298 K.[15] The temperature dependence of σ_{BrO} at the (9,0) band head was estimated to be $\sigma_{BrO} = 1.6$, 1.5, 1.4, 1.2, 1.1, and 1.0×10^{-17} cm^2 molecule^{-1} at 233, 253, 273, 293, 313, and 333 K, respectively, assuming the same temperature dependence as for the (7, 0) band head.[16] This assumption was supported by spectrum simulations with reported molecular constants and an appropriate spectrum width caused by predissociation. Considering uncertainties in σ_{BrO}, pressure, mass flow rates, reaction path length, and fluctuation of the photolysis laser power, we estimate the uncertainty in the BrO concentration is approximately 23%.

By varying the delay between the photolysis and the probe laser pulses, the concentration of BrO was monitored as a function of delay time. The BrO concentration profile was measured 0.1−20 ms after the photolysis laser pulse. Ozone concentrations were measured upstream of the reaction tube by monitoring the absorption at 253.7 nm using a separate low-pressure Hg lamp as a light source with $\sigma_{O3} = 1.15 \times 10^{-17}$ cm^2 molecule^{-1}.[15] The temperature of the gas flow region was controlled over the range 233−333 K by circulating ethanol or water through a jacket surrounding the reaction cell. The difference between the temperature of the sample gas at the entrance and that at the exit of the flow region was <1 K. The pressure in the cell was monitored by an absolute pressure gauge (Copal, PA830). To minimize deterioration of mirrors caused by exposure to the reactants and products, a slow flow of nitrogen gas was introduced at both ends of the ring-down cavity, close to the mirrors. The total flow rate (typically 2000 sccm) was adjusted so that the gas in the cell was replaced completely within the 0.5 s time interval between photolysis laser pulses. Diluted C_2H_5Br/O_2 sample mixtures were prepared in glass bulbs and introduced into the reaction cell using mass flow controllers (STEC, SECE40). Concentrations of reactants were calculated from measured flow rates. All reagents were obtained from commercial sources. C_2H_5Br (>99%, Kishida Chemicals Co) was subjected to freeze−pump−thaw cycling before use. N_2 (>99.999%) and O_2 (>99.995%) were used as received.

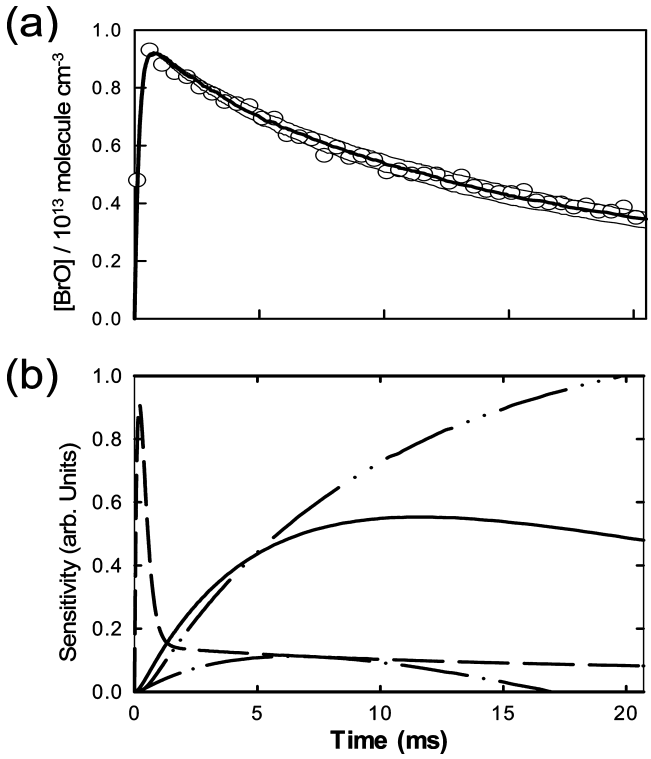

Figure 2. (a) Typical BrO profile for an experiment conducted at 293 K and 150 Torr total pressure of O_2 diluent with $[C_2H_5Br] = 6.2 \times 10^{15}$, $[O_3] = 4.6 \times 10^{15}$, $[Br]_0 = [C_2H_5]_0 = 9.8 \times 10^{12}$, and $[O]_0 = 1.5 \times 10^{13}$ molecules cm^{-3}. The thick and thin curves show simulations using $k_6 = (4.1 \pm 1.0) \times 10^{-12}$ cm^3 molecule^{-1} s^{-1}. (b) Sensitivity analysis with CHEMKIN II for temporal changes of [BrO]; BrO + $C_2H_5O_2$ → products (solid line), Br + O_3 → BrO + O_2 (dashed line), 2 BrO → 2 Br + O_2 (dashed and double dotted line) and diffusion (dashed and dotted line).

3. Results

3.1. Measurements of k_6. Figure 2a shows a typical BrO rise and decay profile obtained using a reaction mixture containing 6.2×10^{15} C_2H_5Br and 4.6×10^{15} molecules cm^{-3} O_3 in 150 Torr total pressure of O_2 diluent at 293 K. Numerical models were constructed using the chemical mechanism and rate data given in Table 1 and were run using the IBM chemical kinetics simulator (CKS). Initial concentrations of $[Br]_0 = [C_2H_5]_0$ were varied to provide the best fit of experimental BrO decay profiles. A weighted average of 8 independent experiments in 150 Torr total pressure of O_2 diluent at 293 K gave $k_6 = (3.8 \pm 1.7) \times 10^{-12}$ cm^3 molecule^{-1} s^{-1}. The quoted uncertainty includes uncertainties in the fit (judged by eye to encompass the noise on experimental data points; see Figure 2a), $[Br]_0$ and $[C_2H_5]_0$, pressure, mass flow rates, reaction path length, and loss of BrO via diffusion and self-reaction. A sensitivity analysis of temporal changes in the BrO concentration was performed using the CHEMKIN II kinetics software package. As shown in Figure 2b, the BrO profile was sensitive to loss via reaction 6, self-reaction, and diffusion. The IUPAC data panel[17] recommended rate constant for the 2 BrO → 2Br + O_2 self-reaction of 2.7×10^{-12} cm^3 molecule s^{-1} was used in the model. As part of our recent study of the BrO + CH_3O_2 reaction,[12] we measured a rate constant of $(2.6 \pm 0.6) \times 10^{-12}$ cm^3 molecule s^{-1} for this reaction in good agreement with the recommended value.

To assess how the decay of BrO radicals might be impacted by the presence of O atoms formed via photolysis of O_3 at 213 nm the initial concentration of O atoms was estimated using the expression:

$$[O]_0 = \frac{\sigma_{O_3}[O_3]}{\sigma_{C_2H_5Br}[C_2H_5Br]}[C_2H_5]_0 \quad (17)$$

Absorption cross sections of $\sigma_{C2H5Br} = 4.5 \times 10^{-19}$ and $\sigma_{O3} = 9.0 \times 10^{-19}$cm^2 molecule^{-1} at 213 nm were taken from the NASA evaluation.[15] The initial O atom concentration was estimated to be $(0.3-1.2) \times 10^{12}$ molecules cm^{-3}. The major fate of O atoms is reaction with O_2 to regenerate O_3. A small fraction (approximately 1% under typical experimental conditions) of O atoms react with $C_2H_5O_2$ radicals leading to a slight delay in the rise of BrO radicals. For completeness, reactions 18−21 were added to the model.

$$O + O_2 + M \rightarrow O_3 + M \quad (18)$$

$$O + C_2H_5O_2 \rightarrow C_2H_5O + O_2 \quad (19)$$

$$C_2H_5O + O_2 \rightarrow HO_2 + CH_3CHO \quad (20)$$

$$BrO + HO_2 \rightarrow HOBr + O_2 \quad (21)$$

Inclusion of these four reactions increased the BrO decay rate by less than 1%. We conclude that the formation of O atoms is not a significant complication in the present experiments.

The concentrations of $C_2H_5O_2$ and BrO radicals were varied by using different initial concentrations of C_2H_5Br. Variation of $[C_2H_5Br]_0$ over the range $(2.5-6.2) \times 10^{15}$ molecules cm^{-3} (corresponding to variation of the maximum concentration of BrO over the range $(3.3-10) \times 10^{12}$ molecules cm^{-3}) had no discernible effect on the value of k_6. Variation of the initial O_3 and O_2 concentrations over the ranges $(2.5-7.0) \times 10^{15}$ and $(0.6-4.9) \times 10^{18}$ molecules cm^{-3} also had no discernible impact on the value of k_6. BrO radicals react slowly, if at all, with O_3[27] and this reaction was not included in the model. By using the chemical mechanism given in Table 1, it was calculated that reaction with $C_2H_5O_2$, self-reaction, and diffusion account for 28, 42, and 18% of the loss of BrO radicals at 2 ms; 29, 40 and 21% at 5 ms; and 31, 36 and 24% at 10 ms, respectively.

Rate data for the potentially complicating secondary reactions Br + $C_2H_5O_2$, Br + C_2H_5O, BrO + C_2H_5O, $C_2H_5O_2$ + O, $C_2H_5O_2$ + C_2H_5, and $C_2H_5O_2$ + C_2H_5O are not available. To estimate the potential impact of these reactions, we used literature data for the analogous reactions for CH_3O_2 (see Table 1). These six reactions were found to contribute less than 1% to the observed loss of BrO radicals.

The effect of absorption by Br_2O (formed in the reaction of Br with BrO) was assessed and found to be negligible because its concentration was calculated to be less than 1×10^{10} molecules cm^{-3} and $\sigma_{Br2O} = 2 \times 10^{-18}$ cm^2 molecule^{-1} at 329.1 nm[28] while $[BrO] = (0.3 - 1) \times 10^{13}$ molecules cm^{-3} and $\sigma_{BrO} = (1.0 - 1.6) \times 10^{-17}$ cm^2 molecule^{-1} over the experimental temperature range. Model simulations showed that the formation of Br_2O_2 was of negligible importance (even at low temperatures) because of the relatively small rate coefficient for the BrO radical association-reaction, $k(BrO + BrO) = 5 \times 10^{-13}$ cm^3 molecule^{-1} s^{-1} at 222 K in 150 Torr of O_2 diluent.[19]

Vibrationally exited BrO radicals, formed from the reaction of Br atom with O_3, were quenched within 2 μs in 50−200 Torr of N_2/O_2 diluent[29] and are not a complication in the present analysis. Photodissociation via excitation to the *A*-band of C_2H_5Br produces ground state Br($^2P_{3/2}$) and spin−orbit excited

TABLE 1: Chemical Mechanisms Used to Simulate the BrO Profile at 293 K and 150 Torr Total Pressure of O_2 Diluent

reaction	rate constant, k_{293} (cm^3 $molecule^{-1}$ s^{-1} or s^{-1})	A (cm^3 $molecule^{-1}$ s^{-1} or s^{-1})	E/R (T)	refs
$Br + O_3 \rightarrow BrO + O_2$	1.1×10^{-12}	1.7×10^{-11}	800	17
$C_2H_5 + O_2 + M \rightarrow C_2H_5O_2 + M$	7.1×10^{-12}	a	a	15
$BrO + C_2H_5O_2 \rightarrow$ products	best-fit parameter	5.1×10^{-13}	−571	this work
$2BrO \rightarrow 2Br + O_2$	2.7×10^{-12}	2.7×10^{-12}	0	17
$\rightarrow Br_2 + O_2$	5.1×10^{-13}	2.9×10^{-14}	−840	17
$2C_2H_5O_2 \rightarrow 2C_2H_5O + O_2$	4.0×10^{-14}	4.0×10^{-14}	0	18
$\rightarrow C_2H_5OH + CH_3CHO + O_2$	2.4×10^{-14}	2.4×10^{-14}	0	18
$C_2H_5O_2 + C_2H_5O \rightarrow$ products	1.0×10^{-12}	1.0×10^{-12}	0	d
$C_2H_5O_2 + HO_2 \rightarrow$ products	8.2×10^{-12}	3.8×10^{-13}	−900	18
$C_2H_5O_2 + C_2H_5 \rightarrow 2C_2H_5O$	2.0×10^{-11}	2.0×10^{-11}	0	e
$C_2H_5O + O_2 \rightarrow HO_2 + CH_3CHO$	9.6×10^{-15}	2.4×10^{-14}	325	18
$C_2H_5O + BrO \rightarrow$ products	5.5×10^{-11}	5.5×10^{-11}	0	f
$Br + BrO + M \rightarrow Br_2O + M$	4.0×10^{-13}	7.7×10^{-34}	−1370	19
$Br + Br_2O \rightarrow Br_2 + BrO$	4.0×10^{-11}	4.0×10^{-11}	0	19
$Br + C_2H_5 \rightarrow C_2H_4 + HBr$	1.2×10^{-11}	1.2×10^{-11}	0	20
$Br + C_2H_5O_2 \rightarrow BrO + C_2H_5O$	4.4×10^{-13}	4.4×10^{-13}	0	g
$Br + C_2H_5O \rightarrow$ products	5.3×10^{-11}	5.3×10^{-11}	0	h
$2Br + M \rightarrow Br_2 + M$	2.2×10^{-14}	b	b	21
$HO_2 + BrO \rightarrow HOBr + O_2$	2.5×10^{-11}	4.5×10^{-12}	−500	17
$HO_2 + Br \rightarrow HBr + O_2$	1.7×10^{-12}	7.7×10^{-12}	450	17
$O + BrO \rightarrow Br + O_2$	4.2×10^{-11}	1.9×10^{-11}	−230	17
$O + O_2 + M \rightarrow O_3 + M$	3.2×10^{-15}	c	c	22
$O + O_3 \rightarrow 2O_2$	7.1×10^{-15}	8.0×10^{-12}	2060	22
$O + Br_2 \rightarrow BrO + Br$	1.5×10^{-11}	5.12×10^{-13}	−989	19
$O + C_2H_5O_2 \rightarrow C_2H_5O + O_2$	4.3×10^{-11}	4.3×10^{-11}	0	i
diffusion rate	20			this work

[a] $k_0 = 1.5 \times 10^{-28}(T/300)^{-3}$ cm^6 $molecule^{-2}$ s^{-1}, $k_\infty = 8.0 \times 10^{-12}$ cm^3 $molecule^{-1}$ s^{-1}. [b] $4.31 \times 10^{-33} \times (T/298)^{-2.77}$ cm^6 $molecule^{-2}$ s^{-1}. [c] $6.0 \times 10^{-34} \times (T/300)^{-2.6}$ cm^6 $molecule^{-2}$ s^{-1}. [d] Adopted from $CH_3O_2 + CH_3O$.[23] [e] Adopted from $CH_3O_2 + CH_3$.[23] [f] Adopted from $CH_3O + BrO$.[24] [g] Adopted from $Br + CH_3O_2$.[25] [h] Adopted from $Br + CH_3O$.[24] [i] Adopted from $O + CH_3O_2$.[26]

$Br^*(^2P_{1/2})$ atoms. In 50−200 Torr of N_2/O_2 diluent, Br* atoms are quenched within 0.3 ms[30] to ground state Br atoms which then react with O_3 to give BrO radicals. Br* atoms would also react directly with O_3 to give BrO radicals. The formation of Br* atoms is not a complication in the present work.

3.2. Pressure Dependence of k_6. To check for a pressure dependence of k_6, experiments were performed using 50, 100, 150, and 200 Torr of O_2/N_2 diluent at 293 K. The maximum concentration of BrO radicals was $(7.0-8.0) \times 10^{12}$ molecules cm^{-3}. Diffusion rate constants of BrO used in the simulation at 293 K were calculated using simple diffusion theory to be 15, 30 and 60 s^{-1} in 200, 100, and 50 Torr, respectively. These values are consistent with our previously reported values.[12,31] Diffusion rate constants for other species (C_2H_5, Br, O and $C_2H_5O_2$) at each pressure were also estimated using simple diffusion theory and included in the model. Averages of 5−8 independent experiments gave values of $k_6 = (4.1 \pm 1.9) \times 10^{-12}$, $(4.2 \pm 1.9) \times 10^{-12}$, $(3.8 \pm 1.7) \times 10^{-12}$ and $(4.3 \pm 1.9) \times 10^{-12}$ cm^3 $molecule^{-1}$ s^{-1} at 50, 100, 150, and 200 Torr, respectively. The quoted uncertainties include uncertainties associated with loss of BrO via self-reaction and diffusion. There was no discernible effect of total pressure on k_6 over the range investigated.

3.3. Temperature Dependence of k_6. Experiments were conducted at 233−333 K in 150 Torr O_2 diluent with maximum concentrations of BrO in the range $(0.6-1.0) \times 10^{13}$ molecules cm^{-3}. Diffusion rate constants of BrO used in model calculations were 14, 16, 18, 22, and 24 s^{-1} at 233, 253, 273, 313, and 333 K, respectively. These values are also consistent with our previously reported values.[12,31] Diffusion rate constants for other species were also estimated at each temperature. The temperature dependence of reactions was accounted for using the literature sources given in Table 1. Values of k_6 determined at 233−333 K are listed in Table 2 and plotted in Figure 3. These values

TABLE 2: Values of $k(BrO + C_2H_5O_2)$ Obtained in 150 Torr Total Pressure of O_2 Diluent at 233−333 K

temperature (K)	$k(BrO + C_2H_5O_2)$ (10^{-12} cm^3 $molecule^{-1}$ s^{-1})
233	5.5 ± 2.0
253	5.0 ± 1.9
273	4.4 ± 1.9
293	3.8 ± 1.7
313	3.3 ± 1.6
333	2.4 ± 1.6

were derived from weighted averages of 6−8 independent experiments and an uncertainty of the diffusion and the self-reaction of BrO. The line through the data in Figure 3 is a weighted fit of the Arrhenius expression which gives $k_6 = 6.5$

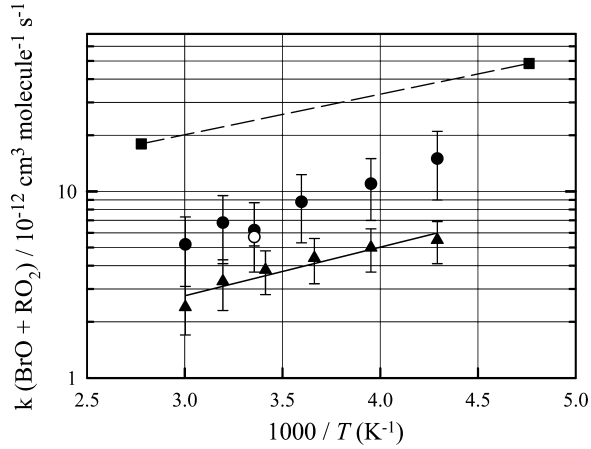

Figure 3. Temperature dependence of the reaction rate constants for BrO with the following: HO_2, squares;[17] CH_3O_2, open circle,[11] filled circles;[12] and $C_2H_5O_2$, triangles (this work).

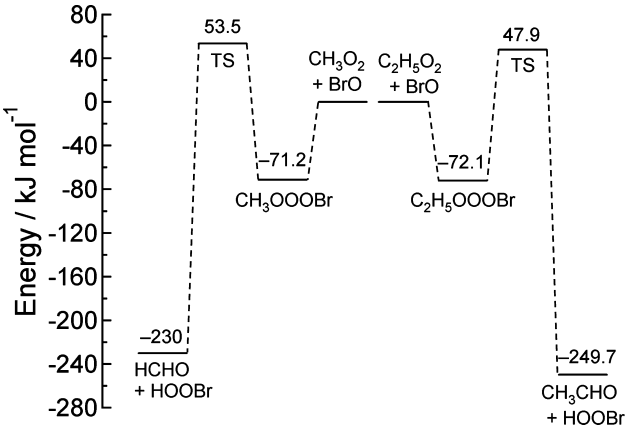

Figure 4. Relative energies for CH_3O_2 + BrO (left half) and $C_2H_5O_2$ + BrO (right half). The energies are calculated at the QCISD(T)/6-311+G(2df,2p) // B3LYP/6-311+G(2df,2p) level of theory.

$\times 10^{-13}$ exp((505 ± 570)/*T*) cm^3 molecule^{-1} s^{-1}. As seen in Figure 3, the reactivity trend is $k(BrO+HO_2) > k(BrO+CH_3O_2) > k(BrO+C_2H_5O_2)$.

3.4. Effect of Water Vapor on k_6. To investigate the possible effect of H_2O on k_6, experiments were performed at 293 K in 150 Torr O_2 diluent with 1.4×10^{17} molecules cm^{-3} of added water vapor. The average of 5 independent experiments in the presence of H_2O vapor and with including uncertainty in the diffusion and the self-reaction of BrO gave $k_6 = (4.0 \pm 1.8) \times 10^{-12}$ cm^3 molecule^{-1} s^{-1}. This result is indistinguishable from that measured in the absence of H_2O vapor, $k_6 = (3.8 \pm 1.7) \times 10^{-12}$ cm^3 molecule^{-1} s^{-1}.

3.5. Theoretical Calculations. Ab initio and density functional theory calculations for reactions 5 and 6 were performed using the Gaussian 03 program.[32] Geometries of reactants, intermediates, transition states, and products were optimized employing the B3LYP/6-311+G(2df,2p) level of theory. Calculated energy diagrams for reactions 5 and 6 are shown in Figure 4. As seen from Figure 4, the relative energies of reactants, adducts, transition states (TS), and products in the two reactions are essentially indistinguishable. Calculated frequencies and geometries are listed in Tables SI and SII in Supporting Information (SI). Total energies were also calculated at the QCISD(T)/6-311+G(2df,2p) // B3LYP/6-311+G(2df,2p) level of theory. Intrinsic reaction coordinate (IRC) calculations were carried out to confirm the connection of the transition states with intermediates and products. Heats of reaction ($\Delta_r H$) are summarized in Tables SIII and SIV in Supporting Information. Relative energies of adducts, TS, and products calculated here are similar to those reported by Guha and Francisco.[13] Differences between our values and those of Guha and Francisco[13] are shown in Table SI−V and reflect differences in levels of theory in the two studies.

4. Discussion

4.1. Effect of H_2O on k_6. The effect of water vapor on kinetics of the self-reaction of HO_2 is well established[33−35] and is explained by the formation of the $HO_2 \cdot H_2O$ complex. Kanno et al. have reported the $HO_2 + H_2O \leftrightarrow HO_2 \cdot H_2O$ equilibrium constant at 297 K and the rate constant for the $HO_2 + HO_2 \cdot H_2O$ reaction.[36] Butkovskaya et al. have shown that the $HO_2 \cdot H_2O$ complex affects the branching ratio for the reaction of HO_2 radicals with NO.[37] Clark et al. suggested that RO_2 radicals may form $RO_2 \cdot H_2O$ complexes, and that the existence of $RO_2 \cdot H_2O$ might perturb the reactivity of RO_2 radicals and consequently affect their kinetics and product branching ratios.[38] Clark et al. calculated that the binding energy of the $C_2H_5O_2 \cdot H_2O$ complex is relatively small, 2.5 kcal mol^{-1}, and suggested that $RO_2 \cdot H_2O$ binding energies >5 kcal mol^{-1} are necessary for such complexes to have an appreciable role in the atmospheric chemistry.[38] The absence of any discernible impact of the presence of 1.4×10^{17} molecules cm^{-3} (4.3 Torr) of H_2O vapor on k_6 at 100 Torr total pressure in the present work is consistent with the small binding energy calculated by Clark et al.[38] for the $C_2H_5O_2 \cdot H_2O$ complex.

4.2. Comparison with Literature Data and Atmospheric Implications. Table 3 summarizes available kinetic data for reactions of ClO, BrO, and IO radicals with HO_2, CH_3O_2, and $C_2H_5O_2$ radicals. As seen from Table 3, the reactions have small or negative temperature dependencies consistent with a reaction mechanism proceeding via the formation of an intermediate complex. The rates of the reactions with HO_2, CH_3O_2, and $C_2H_5O_2$ increase in the order $k(ClO) < k(BrO) < k(IO)$. The same trend is evident in self-reaction rate constants of ClO, BrO, and IO radicals,[14] and has been rationalized in terms of decreasing ionization potentials; 10.9 eV for ClO, 10.5 eV for BrO, and 9.7 eV for IO.[12]

The negative temperature dependence of rate constants for BrO + RO_2 (R = H, CH_3, C_2H_5) has been attributed to a reaction mechanism which proceeds via the formation of an intermediate complex:

$$BrO + RO_2 \rightarrow \text{adduct} \rightarrow \text{transition state} \rightarrow \text{products} \quad (22)$$

Guha and Francisco concluded from their theoretical calculations that the intermediates in the BrO + HO_2 reaction are HOOOBr and HOOBrO.[41]

$$BrO + HO_2 \rightarrow HOOOBr \rightarrow TS \rightarrow HOBr + O_2 \quad (23)$$

$$BrO + HO_2 \rightarrow HOOBrO \rightarrow TS \rightarrow HOBr + O_2 \quad (24)$$

There are six possible reaction pathways for the reaction 5:

			$\Delta_r H$ (kJ mol^{-1})	
$BrO + CH_3O_2$	→	$CH_3O + BrOO$	-3.5	(25)
	→	$CH_3O + OBrO$	52.4	(26)
	→	$HOBr + CH_2O_2$	-0.9	(27)
	→	$CH_3OBr + O_2$	-206.7	(28)
	→	$HCHO + HOOBr$	-218.4	(29)
	→	$HCHO + O_2 + HBr$	-273.6	(30)

Thermochemical data for reactions 28 and 29 were taken from Guha and Francisco.[13] $\Delta H_f(CH_2O_2)$ was taken from Aranda et al.[11] Guha and Francisco[13] concluded that the most feasible pathway for the CH_3O_2 + BrO reaction is formation of the CH_3OOOBr intermediate followed by dissociation into HCHO + HOOBr.[13]

$$BrO + CH_3O_2 \rightarrow CH_3OOOBr \rightarrow \text{four-membered TS} \rightarrow HCHO + HOOBr \quad (31)$$

TABLE 3: Summary of Rate Constants of XO + RO_2

	rate constant (cm^3 $molecule^{-1}$ s^{-1})		
XO	HO_2	CH_3O_2	$C_2H_5O_2$
ClO	2.2×10^{-12} exp(340/*T*),[17] $k_{298} = 6.9 \times 10^{-12}$	2.4×10^{-12} exp(−20/*T*),[39] $k_{298} = 2.2 \times 10^{-12}$	
BrO	4.5×10^{-12} exp(500/*T*),[17] $k_{298} = 2.4 \times 10^{-11}$	4.6×10^{-13} exp(798/*T*),[11] $k_{298} = 6.7 \times 10^{-12}$	6.5×10^{-13} exp(505/*T*) $k_{298} = 3.5 \times 10^{-12}$
IO	1.4×10^{-11} exp(540/*T*),[17] $k_{298} = 8.6 \times 10^{-11}$	1.3×10^{-10} exp(−168/*T*),[40] $k_{298} = 7.4 \times 10^{-11}$	$k_{298} = 1.4 \times 10^{-10}$,[40]

As with the BrO + CH_3O_2 reaction, six reaction pathways are possible for the BrO + $C_2H_5O_2$ reaction as shown in the introduction section. In the present theoretical study, we show (see Figure 4) that essentially the same pathway leading to aldehyde and HOOBr via the ROOOBr intermediate exists in the reactions of CH_3O_2 and $C_2H_5O_2$ with BrO. Building on the work by Guha and Francisco[13] for CH_3O_2, we conclude that it is likely that the reaction of $C_2H_5O_2$ with BrO proceeds mainly via:

$$\mathrm{BrO} + \mathrm{C_2H_5O_2} \rightarrow \mathrm{C_2H_5OOOBr} \rightarrow \text{four-membered TS} \rightarrow \mathrm{CH_3CHO} + \mathrm{HOOBr} \quad (32)$$

Rate constants reported here and in our previous study[12] describe the kinetics of BrO radicals in the system which include loss via reaction with RO_2 radicals and regeneration via dissociation of ROOOBr.

$$\mathrm{BrO} + \mathrm{RO_2} \underset{k_{-a}}{\overset{ka}{\rightleftharpoons}} \mathrm{ROOOBr} \rightarrow \text{products} \quad (33)$$

The overall loss of BrO is given by

$$-\frac{\mathrm{d[BrO]}}{\mathrm{d}t} = k_a[\mathrm{BrO}][\mathrm{RO_2}] - k_{-a}[\mathrm{ROOOBr}] \quad (34)$$

The absence of any discernible effect of total pressure on k(BrO + $C_2H_5O_2$) reported here and k(BrO + CH_3O_2)[12] indicates that dissociation of ROOOBr to RO_2 + BrO is negligible. Then, eq 33 can be modified as

$$-\frac{\mathrm{d[BrO]}}{\mathrm{d}t} \approx k_a[\mathrm{BrO}][\mathrm{RO_2}] \quad (35)$$

This suggests that the observed rate constant for BrO loss is determined by the potential energy surface (PES) at the entrance channel, BrO + RO_2 →ROOOBr. Differences between rate constants of reactions 5 and 6 would then reflect differences in the PES at the entrance channel. We can not compare the kinetics of reaction 4 to those of reaction 2 in a similar manner, since it is believed that reaction 2 proceeds via both HOOOBr and HOOBrO intermediates, which is a different mechanism from that of reaction 4.

The goal of the present work was to extend the kinetic database for reactions of BrO radicals with organic peroxy radicals. Specifically, we wished to address the question of whether the reactivity of BrO toward CH_3O_2 radicals is representative of the reactivity of BrO toward the mixture of organic peroxy radicals found in the atmosphere. As seen from Figure 3, over the temperature range studied the reactivity of BrO radicals toward $C_2H_5O_2$ radicals is comparable in magnitude and temperature dependence to, but approximately a factor of 2 lower than, that toward CH_3O_2. As discussed previously,[12] there are relatively few simultaneous measurements of RO_2 and HO_2 radicals in, or near, marine environments where BrO radical levels may be significant. Measurements at Mace Head, Ireland, on 31st July 1996 of [RO_2] by Salisbury et al.[8] and [HO_2] by Creasey et al.[9] indicate that at local noon the [RO_2 + HO_2] concentration is approximately 60 ppt while the HO_2 concentration is approximately 10 ± 5 ppt. The MCM box model study reported by Sommariva et al. also indicates that the maximum RO_2 concentration is approximately 60 ppt, while the HO_2 concentration is approximately 10 ppt.[10] Equating k_4 with the average of the values of k_5 from Aranda et al.[11] and Enami et al.[12] (calculated at 298 K from the Arrhenius expression) and k_6 from the present work (calculated at 298 K from the Arrhenius expression) gives $k_4/k_2 = 4.9 \times 10^{-12}/2.4 \times 10^{-11} = 0.2$.[17] Taking [$RO_2$]/[$HO_2$] = 3−11 gives $k_4[\mathrm{RO_2}]/k_2[\mathrm{HO_2}] = 0.6-2.2$. It seems clear that reaction with organic peroxy radicals will be an important loss mechanism for BrO radicals in the troposphere and should be included in global atmospheric models of tropospheric ozone chemistry. Further work is needed to clarify the mechanism and products of reaction 4 and to establish whether substituted organic peroxy radicals (e.g., $CH_3C(O)O_2$) react any differently than alkylperoxy radicals.

Conclusions

The rate coefficient for the BrO + $C_2H_5O_2$ reaction was measured at 233−333 K in 50−200 Torr of O_2 diluent. The rate coefficient had a negative temperature dependence suggesting that the reaction proceeds via the formation of an intermediate complex. There was no discernible dependence of the rate of reaction on total pressure indicating that dissociation of an intermediate complex to reform reactants BrO and $C_2H_5O_2$ is negligible over the 50−200 Torr range studied.

The present theoretical result shows that the $C_2H_5O_2$ + BrO reaction proceeds via pathways similar to those for the CH_3O_2 + BrO reaction; that is, (1) the most plausible pathway for the $C_2H_5O_2$ + BrO reaction results in production of CH_3CHO and HOOBr including the formation of C_2H_5OOOBr as an intermediate complex, and (2) no significant Br reformation occurs. Calculated energies are also similar to those for CH_3O_2 + BrO, suggesting that rate constants for RO_2 + BrO reactions are controlled by the potential energy surface at the entrance channel to form intermediate species.

Combining the reported tropospheric mixing ratios for HO_2 and RO_2[8−10] with kinetic data for reactions of BrO with HO_2 and RO_2 radicals from the present and previous studies[10,11,17] indicates that the RO_2 + BrO reaction will be significant in the atmosphere. Such reactions should be included in future global atmospheric models of tropospheric ozone chemistry.

Acknowledgment. This work was supported in part by Grants-in-Aid for Scientific Research from the Ministry of Education, Culture, Sports, Science and Technology (19350004 and 20245005).

Supporting Information Available: Results of theoretical calculations. This information is available free of charge via the Internet at http://pubs.acs.org.

References and Notes

(1) Saiz-Lopez, A.; Plane, J. M. C.; Shillito, J. A. *Geophys. Res. Lett.* **2004**, *31*, L03111.

(2) Kreher, K.; Johnston, P.; Wood, S. W.; Nardi, B.; Platt, U. *Geophys. Res. Lett.* **1997**, *24*, 3021.

(3) Tas, E.; Peleg, M.; Matveev, V.; Zingler, J.; Luria, M. *J. Geophys. Res.* **2005**, *110*, D11304.

(4) Fitzenberger, R.; Bösch, H.; Camy-Peyret, C.; Chipperfield, M.; Harder, H.; Platt, U.; Sinnhuber, B.-M.; Wagner, T.; Pfeilsticker, K. *Geophys. Res. Lett.* **2000**, *27*, 2921.

(5) Read, K. A.; Mahajan, A. S.; Carpenter, L. J.; Evans, M. J.; Faria, B. V. E.; Heard, D. E.; Hopkins, J. R.; Lee, J. D.; Moller, S. J.; Lewis, A. C.; Mendes, L.; McQuaid, J. B.; Oetjen, H.; Saiz-Lopez, A.; Pilling, M. J.; Plane, J. M. C. *Nature* **2008**, *453*, 1232.

(6) von Glasow, R.; von Kuhlmann, R.; Lawrence, M. G.; Platt, U.; Crutzen, P. J. *Atmos. Chem. Phys.* **2004**, *4*, 2481.

(7) Yang, X.; Cox, R. A.; Warwick, N. J.; Pyle, J. A.; Carver, G. D.; O'Connor, F. M.; Savage, N. H. *J. Geophys. Res.* **2005**, *110*, D23311.

(8) Salisbury, G.; Monks, P. S.; Bauguitte, S.; Bandy, B. J.; Penkett, S. A. *J. Atmos. Chem.* **2002**, *41*, 163.

(9) Creasey, D. J.; Halford-Maw, P. A.; Heard, D. E.; Pilling, M. J.; Whitaker, B. J. *J. Chem. Soc., Faraday Trans.* **1997**, *93*, 2907.

(10) Sommariva, R.; Osthoff, H. D.; Brown, B. B.; Bates, T. S.; Baynard, T.; Coffman, D.; de Gouw, J. A.; Goldan, P. D.; Kuster, W. C.; Lerner, B. M.; Stark, H.; Warneke, C.; Williams, E. J.; Fehsenfeld, F. C.; Ravishankara, A. R.; Trainer, M. *Atmos. Chem. Phys.* **2009**, *9*, 3075.

(11) Aranda, A.; LeBras, G.; LaVerdet, G. L.; Poulet, G. *Geophys. Res. Lett.* **1997**, *24*, 2745.

(12) Enami, S.; Yamanaka, T.; Nakayama, T.; Hashimoto, S.; Kawasaki, M.; Shallcross, D. E.; Nakano, Y.; Ishiwata, T. *J. Phys. Chem. A* **2007**, *111*, 3342.

(13) Guha, S.; Francisco, J. S. *J. Chem. Phys.* **2003**, *118*, 1779.

(14) Atkinson, R.; Baulch, D. L.; Cox, R. A.; Hampson, R. F.; Kerr, J. A.; Rossi, M. J.; Troe, J. *J. Phys. Chem. Ref. Data,* **2000**, *29*, 167.

(15) Sander, S. P.; Friedl, R. R.; Ravishankara, A. R.; Golden, D. M.; Kolb, C. E.; Kurylo, M. J.; Huie, R. E.; Orkin, V. L.; Molina, M. J.; Moortgat, G. K.; Finlayson-Pitts, B. J. *Chemical Kinetics and Photochemical Data for Use in Stratospheric Modeling; Evaluation 15*; Jet Propulsion Laboratory: Pasadena, CA, 2006.

(16) Gilles, M. K.; Turnipseed, A. A.; Burkholder, J. B.; Ravishankara, A. R.; Solomon, S. *J. Phys. Chem. A* **1997**, *101*, 5526.

(17) Atkinson, R.; Baulch, D. L.; Cox, R. A.; Crowley, J. N.; Hampson, R. F.; Hynes, R. G.; Jenkin, M. E.; Rossi, M. J.; Troe, J. *Atmos. Chem. Phys.* **2007**, *7*, 981.

(18) Atkinson, R.; Baulch, D. L.; Cox, R. A.; Crowley, J. N.; Hampson, R. F.; Hynes, R. G.; Jenkin, M. E.; Rossi, M.; Troe, J. *Atmos. Chem. Phys.* **2006**, *6*, 3625.

(19) Harwood, M. H.; Rowley, D. M.; Cox, R. A.; Jones, R. L. *J. Phys. Chem. A* **1998**, *102*, 1790.

(20) Dobis, O.; Benson, S. W. *J. Phys. Chem. A* **1997**, *101*, 6030.

(21) Donohoue, D. L.; Bauer, D.; Cossairt, B. A.; Hynes, J. *J. Phys. Chem. A* **2006**, *110*, 6623.

(22) Atkinson, R.; Baulch, D. L.; Cox, R. A.; Crowley, J. N.; Hampson, R. F.; Hynes, R. G.; Jenkin, M. E.; Rossi, M. J.; Troe, J. *Atmos. Chem. Phys.* **2004**, *4*, 1461.

(23) Bale, C. S. E.; Canosa-Mas, C. E.; Shallcross, D. E.; Wayne, R. P. *Phys. Chem. Chem. Phys.* **2005**, *7*, 2164.

(24) Shah, D.; Canosa-Mas, C. E.; Hendy, N. J.; Scott, M. J.; Vipond, A.; Wayne, R. P. *Phys. Chem. Chem. Phys.* **2001**, *3*, 4932.

(25) Francisco, J. S.; Crowley, J. N. *J. Phys. Chem. A* **2006**, *110*, 3778.

(26) Zellner, R.; Hartmann, D.; Karthauser, J.; Rhasa, D.; Weibring, G. *J. Chem. Soc., Faraday Trans. 2* **1988**, *84*, 549.

(27) Rattigan, O. V.; Cox, R. A.; Jones, R. L. *J. Chem. Soc., Faraday Trans.* **1995**, *91*, 4189.

(28) Deters, B.; Burrows, J. P.; Himmelmann, S.; Blindauer, C. *Ann. Geophys.* **1996**, *14*, 468.

(29) Ninomiya, Y.; Hashimoto, S.; Kawasaki, M.; Wallington, T. J. *Int. J. Chem. Kinet.* **2000**, *32*, 125.

(30) Johnson, R. O.; Perram, G. P.; Roh, W. B. *J. Chem. Phys.* **1996**, *104*, 7052.

(31) Nakano, Y.; Goto, M.; Hashimoto, S.; Kawasaki, M.; Wallington, T. J. *J. Phys. Chem. A* **2001**, *105*, 11045.

(32) Frisch, M. J.; Trucks, G. W.; Schlegel, H. B.; Scuseria, G. E.; Robb, M. A.; Cheeseman, J. R.; Montgomery, J. A., Jr.; Vreven, T.; Kudin, K. N.; Burant, J. C.; Millam, J. M.; Iyengar, S. S.; Tomasi, J.; Barone, V.; Mennucci, B.; Cossi, M.; Scalmani, G.; Rega, N.; Petersson, G. A.; Nakatsuji, H.; Hada, M.; Ehara, M.; Toyota, K.; Fukuda, R.; Hasegawa, J.; Ishida, M.; Nakajima, T.; Honda, Y.; Kitao, O.; Nakai, H.; Klene, M.; Li, X.; Knox, J. E.; Hratchian, H. P.; Cross, J. B.; Bakken, V.; Adamo, C.; Jaramillo, J.; Gomperts, R.; Stratmann, R. E.; Yazyev, O. ; Austin, A. J.; Cammi, R.; Pomelli, C.; Ochterski, J. W.; Ayala, P. Y.; Morokuma, K.; Voth, G. A.; Salvador, P.; Dannenberg, J. J.; Zakrzewski, V. G.; Dapprich, S.; Daniels, A. D.; Strain, M. C.; Farkas, O.; Malick, D. K.; Rabuck, A. D.; Raghavachari, K.; Foresman, J. B.; Ortiz, J. V.; Cui, Q.; Baboul, A. G.; Clifford, S.; Cioslowski, J.; Stefanov, B. B.; Liu, G.; Liashenko, A.; Piskorz, P.; Komaromi, I.; Martin, R. L.; Fox, D. J.; Keith, T.; Al-Laham, M. A.; Peng, C. Y.; Nanayakkara, A.; Challacombe, M.; Gill, P. M. W.; Johnson, B.; Chen, W.; Wong, M. W.; Gonzalez, C.; Pople, J. A. *Gaussian 03*, revision C.02; Gaussian, Inc.: Wallingford, CT, 2004.

(33) Hamilton, E. J., Jr. *J. Chem. Phys.* **1975**, *63*, 3826.

(34) Lii, R.-R.; Sauer, M. C., Jr.; Gordon, S. *J. Phys. Chem.* **1981**, *85*, 2833.

(35) Kircher, C. C.; Sander, S. P. *J. Phys. Chem.* **1984**, *88*, 2082.

(36) Kanno, N.; Tonokura, K.; Tezaki, A.; Koshi, M. *J. Phys, Chem, A* **2005**, *109*, 3153.

(37) Butkovskaya, N. I.; Kukui, A.; Pouvesle, N.; Le Bras, G. *J. Phys Chem. A* **2005**, *109*, 6509.

(38) Clark, J.; English, A. M.; Hansen, J. C.; Francisco, J. S. *J. Phys. Chem. A* **2008**, *112*, 1587.

(39) Atkinson, R.; Baulch, D. L.; Cox, R. A.; Crowley, J. N.; Hampson, R. F.; Hynes, R. G.; Jenkin, M. E.; Rossi, M. J.; Troe, J.; Wallington, T. J. *Atmos. Chem. Phys.* **2008**, *8*, 4141.

(40) Enami, S.; Yamanaka, T.; Hashimoto, S.; Kawasaki, M.; Nakano, Y.; Ishiwata, T. *J. Phys. Chem. A* **2006**, *110*, 9861.

(41) Guha, S.; Francisco, J. S. *J. Phys. Chem. A* **1999**, *103*, 8000.

JP904529A